Journal of Clinical and Translational Hepatology **2026**
DOI: 10.14218/JCTH.2025.00666

Original Article

Single-cell Sequencing Reveals Neutrophil Extracellular Traps in Association with Endotheliopathy and Immunothrombosis in Hepatitis B Virus-related Acute-on-chronic Liver Failure

Xitang Li[1,2], Suping Hai[1], Xizhe Zheng[1], Peng Hu[1], Wenhui Wu[1], Qiang Gao[1], Junjian Hu[1], Binghui Yu[1], Feiyang Xu[1], Huiling Xiang[1], Qin Ning[1*] and Xiaojing Wang[1*]

[1]*Department of Infectious Diseases, Tongji Hospital, Tongji Medical College and State Key Laboratory for Diagnosis and Treatment of Severe Zoonotic Infectious Diseases, Huazhong University of Science and Technology, Wuhan, Hubei, China;* [2]*Key Laboratory for Zoonosis Research of the Ministry of Education, Jilin University, Changchun, Jilin, China*

Received: December 05, 2025 | **Revised:** February 19, 2026 | **Accepted:** March 27, 2026 | **Published online:** April 10, 2026

Abstract

Background and Aims: Immunothrombosis, the interplay between immune activation and coagulation, contributes to disease progression in inflammatory disorders. Its role in hepatitis B virus–related acute-on-chronic liver failure (HBV-ACLF) and the involvement of neutrophil extracellular traps (NETs) remain unclear. This study aimed to elucidate NETs-mediated immunothrombosis in HBV-ACLF. ***Methods:*** Liver single-cell RNA sequencing data from HBV-ACLF patients and healthy controls were analyzed to define immune and endothelial transcriptional profiles. A cohort of 46 HBV-ACLF patients, 20 chronic hepatitis B patients, and 20 healthy controls was assessed for circulating NETs, endothelial injury markers, and coagulation parameters. Histopathology and *in vitro* assays examined NETs distribution and endothelial interactions. ***Results:*** NETs were markedly elevated in HBV-ACLF and correlated with endothelial injury markers (syndecan-1, von Willebrand factor, soluble thrombomodulin), coagulopathy, and prognostic scores. Histology revealed NETs colocalization with endothelial cells and platelets within hepatic microthrombi. NETs from patient neutrophils impaired endothelial integrity and enhanced procoagulant activity *in vitro*. Mechanistically, toll-like receptor 2 (TLR2) and complement component 5a receptor 1 (C5aR1) signaling were involved in NETs formation, and their pharmacological inhibition reduced NETs generation. ***Conclusions:*** NETs are associated with endothelial injury and immunothrombosis in HBV-ACLF. Mechanistic analyses suggest a role for TLR2 and C5aR1 pathways in NETs formation, indicating potential targets for future therapeutic investigation.

Keywords: Immunothrombosis; Neutrophil extracellular traps; NETs; Hepatitis B virus–related acute-on-chronic liver failure; HBV-ACLF; Endothelial dysfunction; Single-cell RNA sequencing.

***Correspondence to:** Xiaojing Wang and Qin Ning, Department of Infectious Diseases, Tongji Hospital, Tongji Medical College and State Key Laboratory for Diagnosis and Treatment of Severe Zoonotic Infectious Diseases, Huazhong University of Science and Technology, Wuhan, Hubei 430030, China. ORCID: https://orcid.org/0000-0002-2027-9593 (QN). Tel/Fax: +86-27-83662391 (QN), E-mail: wxjmoon@hotmail.com (XW) and qning@vip.sina.com (QN).

Citation of this article: Li X, Hai S, Zheng X, Hu P, Wu W, Gao Q, *et al*. Single-cell Sequencing Reveals Neutrophil Extracellular Traps in Association with Endotheliopathy and Immunothrombosis in Hepatitis B Virus-related Acute-on-chronic Liver Failure. J Clin Transl Hepatol 2026. doi: 10.14218/JCTH.2025.00666.

Introduction

Hepatitis B virus-related acute-on-chronic liver failure (HBV-ACLF) is a life-threatening clinical syndrome characterized by rapid deterioration of liver function and multi-organ failure. Its short-term mortality rate is as high as 74.6%, which is significantly higher than that observed in liver failure of other etiologies.[1,2] Currently, the main treatments for HBV-ACLF include antiviral therapy and supportive care, but the therapeutic effect remains limited, and no effective immunomodulatory targets have been established.[3] There is thus an urgent need to clarify the underlying pathogenic mechanisms of HBV-ACLF and identify novel therapeutic targets.

A hallmark of HBV-ACLF is the concurrent presence of immune dysregulation and coagulation abnormalities.[1,4] Previously viewed as independent pathophysiological processes, accumulating evidence now indicates that innate immune activation can directly initiate and propagate coagulation through a process termed "immunothrombosis".[5] Characterized by dynamic crosstalk among immune cells and components of the coagulation cascade, immunothrombosis emerges early in disease progression and contributes to microvascular thrombosis, tissue ischemia, and ultimately multiorgan dysfunction.[6–9] In systemic inflammatory conditions such as sepsis and COVID-19, immunothrombosis has been established as a central mediator of organ injury. Therapeutic interventions targeting key molecular effectors of this pathway have yielded organ-protective benefits without significantly increasing the risk of systemic hemorrhage.[10,11] Similarly, HBV-ACLF is characterized by intense systemic inflammation—including cytokine storm and hyperactivation of neutrophils and

Copyright: © 2026 The Author(s). This article has been published under the terms of Creative Commons Attribution-Noncommercial 4.0 International License (CC BY-NC 4.0), which permits noncommercial unrestricted use, distribution, and reproduction in any medium, provided that the following statement is provided. "This article has been published in *Journal of Clinical and Translational Hepatology* at https://doi.org/10.14218/JCTH.2025.00666 and can also be viewed on the Journal's website at http://www.jcthnet.com".

macrophages[12]—as well as marked coagulation disturbances, such as prolonged international normalized ratio (INR), elevated D-dimer levels, and intrahepatic fibrin deposition.[6,13] Nevertheless, despite this striking co-occurrence of immune activation and coagulopathy, the extent to which immune cells directly contribute to intrahepatic microthrombus formation in HBV-ACLF remains incompletely elucidated.

Neutrophil extracellular traps (NETs) have emerged as a central mediator of immunothrombosis.[14,15] NETs are web-like structures composed of decondensed chromatin decorated with granular antimicrobial proteins, which are released by activated neutrophils.[16] Beyond their antimicrobial functions, NETs exert cytotoxic effects on vascular endothelial cells and serve as a prothrombotic scaffold that facilitates platelet adhesion and aggregation, as well as thrombin generation.[14,17] Liver sinusoidal endothelial cells (LSEC) are especially susceptible to NETs-mediated injury. Under physiological conditions, LSEC maintain a non-adhesive and anticoagulant phenotype; disruption of this homeostatic state can profoundly impair intrahepatic microcirculation and coagulation balance.[18] Although endothelial dysfunction is increasingly recognized as a hallmark feature of HBV-ACLF, a comprehensive and functionally integrated characterization of endothelial injury in this disease remains lacking.

Existing evidence on endothelial injury in HBV-ACLF remains fragmented. Although prior studies have reported elevated circulating thrombomodulin levels[19] and alterations in specific endothelial subsets,[20] these findings do not fully capture the multidimensional nature of endothelial dysfunction. Endothelial damage encompasses glycocalyx degradation (syndecan-1), endothelial activation with hemostatic imbalance (von Willebrand factor [vWF] and soluble thrombomodulin [sTM]), and elevated inflammatory adhesion molecule expression (intercellular adhesion molecule-1 [ICAM-1])[18]; however, these dimensions have rarely been examined systematically in relation to NETs formation and clinical outcomes in HBV-ACLF. This knowledge gap limits mechanistic insight into how innate immune activation may drive intrahepatic immunothrombosis.

We therefore hypothesize that excessive NETs may contribute to the multifaceted endothelial injury and immunothrombosis in HBV-ACLF, a mechanism unexplored in this context. To test this, we conducted an integrated study quantifying circulating NETs and a panel of endothelial injury biomarkers in patients and correlating them with clinical outcomes, visualizing their spatial co-localization in liver tissue, and performing functional *in vitro* assays to explore upstream signaling pathways. This study aimed to define the relationship between NETs formation and endothelial injury in HBV-ACLF and explore potential underlying mechanisms.

Methods

Study subjects and inclusion/exclusion criteria

A total of 46 HBV-ACLF patients and 20 chronic hepatitis B (CHB) patients were consecutively enrolled in this study. All participants were admitted to Tongji Hospital, Tongji Medical College, Huazhong University of Science and Technology between August 2021 and May 2022. In addition, 20 healthy controls (HC) were recruited during the same period. The inclusion criteria were as follows: (1) Chronic HBV infection—defined as persistent positivity for hepatitis B surface antigen and/or detectable HBV DNA for ≥6 months[21]; (2) Diagnosis of HBV-ACLF—meeting the Asian Pacific Association for the Study of the Liver (APASL) diagnostic criteria at admission: total bilirubin (TBil) ≥ 5 mg/dL and coagulopathy (INR ≥ 1.5 or prothrombin activity [PTA] < 40%).[22]

The exclusion criteria were as follows: age <18 or >80 years; pregnancy; chronic liver disease attributable to non-HBV etiologies (e.g., alcoholic liver disease) or concurrent infection with non-HBV hepatotropic viruses (e.g., hepatitis A virus or hepatitis C virus); presence of hepatic or extrahepatic malignancy; severe extrahepatic organic disease; use of immunosuppressive agents for the management of extrahepatic organic disease; death within 48 h of hospital admission, voluntary discharge against medical advice, or receipt of liver transplantation; missing key clinical data; or loss to follow-up.

Bacterial infection was diagnosed in accordance with the APASL guidelines[23] and established clinical criteria, integrating clinical symptoms, laboratory parameters, radiological findings, and/or microbiological evidence documented either at admission or during hospitalization. Common bacterial infections included spontaneous bacterial peritonitis, urinary tract infection, pneumonia, spontaneous bacteremia, and skin and soft tissue infection, consistent with those reported in prior studies of ACLF.

Liver tissue samples were obtained from five patients with HBV-ACLF who underwent liver transplantation. Human liver specimens from patients with benign hepatic hemangioma served as HC. All liver samples were immediately fixed in 4% paraformaldehyde upon collection for subsequent analyses. Written informed consent was obtained from all participants prior to enrollment. This study was reviewed and approved by the Ethics Committee of Tongji Hospital, Tongji Medical College, Huazhong University of Science and Technology (approval no. 2021S125).

Clinical data collection

Baseline clinical data were collected from all enrolled patients, including: (1) demographic characteristics (e.g., age and sex); (2) medical history (including past medical conditions and current illness); (3) clinical manifestations; (4) laboratory parameters—namely, complete blood count, routine biochemical tests, hepatitis B e antigen status, HBV DNA viral load, imaging findings, and microbiological test results; and (5) survival outcomes—specifically, 28-day and 90-day survival rates. Patients diagnosed with HBV-ACLF were categorized as survivors or non-survivors based on their vital status at day 90 post-enrollment.

Prognostic scoring systems were calculated using baseline variables: the Chinese Group on the Study of Severe Hepatitis B–ACLF II (COSSH-ACLF II) score was computed according to the validated formula: COSSH-ACLF II = 1.649 × ln (INR) + 0.457 × hepatic encephalopathy score + 0.425 × ln [neutrophil count ($\times 10^9$/L)] + 0.396 × ln [TBil (μmol/L)] + 0.576 × ln [blood urea nitrogen (mmol/L)] + 0.033 × age. Risk stratification was defined as follows: low risk (<7.4), intermediate risk (7.4–8.4), and high risk (>8.4).[24] Model for End-Stage Liver Disease (MELD) score and MELD-sodium (MELD-Na) score were calculated using the standard formulas established in the literature.[25,26]

Acquisition and processing of Single-cell RNA sequencing (scRNA-seq) data

The scRNA-seq data analyzed in this study were retrieved from the public dataset PRJNA913603 (NCBI Sequence Read Archive, SRA), generated by the Third Xiangya Hospital.[20] A total of nine scRNA-seq samples were included: five from patients with HBV-ACLF (samples ACLF1–ACLF5) and four from HC (HC1–HC4). Raw sequencing reads were aligned to the human reference genome (GRCh38) and quantified at the gene level using Cell Ranger (v6.1.2).[27] Downstream analy-

ses were performed in Seurat (v4.3.0).[28] For quality control at the single-cell level, cells expressing fewer than 500 unique genes or exhibiting mitochondrial gene content exceeding 20% were excluded. Additionally, genes detected in fewer than 10 cells across the entire dataset were filtered out.

Following quality filtering, the number of retained cells per sample ranged from 3,425 to 11,824. Median UMI counts, numbers of detected genes, and mitochondrial gene percentages exhibited comparable distributions across all samples. Specifically, median mitochondrial gene percentages ranged from 4.8% to 6.7%, with consistent interquartile ranges—indicating high reproducibility and overall uniform data quality between HBV-ACLF and HC samples. Gene expression counts were normalized using SCTransform, and highly variable genes were identified for downstream integration. Data integration across samples was performed using Seurat's anchor-based integration workflow, leveraging shared highly variable genes to correct for batch effects. Integrated data were subsequently scaled using ScaleData prior to dimensionality reduction.[29] Principal component analysis was applied to the integrated dataset,[30] followed by graph-based clustering using the Louvain algorithm and nonlinear visualization via t-distributed stochastic neighbor embedding. Cell types were annotated based on established canonical marker genes.

Isolation of peripheral blood neutrophils

Peripheral blood neutrophils were isolated using a commercial neutrophil isolation kit (Solarbio, Cat. No. 9040).[31] Briefly, peripheral blood was carefully layered over Reagent A and Reagent C, respectively, following the manufacturer's instructions. Following centrifugation, neutrophils located at the lower interface were collected, washed twice with phosphate-buffered saline (PBS), and resuspended in appropriate medium for subsequent experiments.

NETs detection

Circulating NETs were quantified by measuring plasma levels of myeloperoxidase (MPO), neutrophil elastase (NE), and MPO–DNA complexes. Plasma MPO and NE concentrations were determined using commercially available enzyme-linked immunosorbent assay (ELISA) kits. Specifically, the Human Myeloperoxidase ELISA Kit (RayBiotech, Cat. No. ELH-MPO) and the Human Neutrophil Elastase ELISA Kit (RayBiotech, Cat. No. ELH-NEUTRO-1) were used according to the manufacturers' protocols. MPO–DNA complexes were detected using a previously established ELISA-based capture method.[32] Briefly, 96-well microtiter plates pre-coated with anti-MPO antibody (supplied in the RayBiotech MPO ELISA kit) were incubated for 2 h at room temperature with diluted plasma samples mixed with horseradish peroxidase-conjugated anti-DNA monoclonal antibody (Component 2 of the Cell Death Detection ELISA Kit; Roche, Basel, Switzerland; Cat. No. 1774425001). Following three washes with PBS, plates were incubated with horseradish peroxidase substrate for 30 min at 37 °C. Absorbance was measured at 450 nm. All samples were analyzed in duplicate, and samples from different study groups were randomly assigned across assay plates to minimize potential batch effects.

Visualization of NETs

Isolated neutrophils (4×10^5 cells/well) were seeded onto polylysine-precoated coverslips and stimulated with plasma from HC, CHB, or HBV-ACLF patients in 12-well plates for 3 h. Neutrophils were also seeded in black 96-well plates with clear, tissue-culture–treated bottoms and incubated with indicated stimuli. SYTOX Green (1 μM) was added to detect extracellular DNA. Fluorescence intensity was quantified using a fluorescence microplate reader (excitation: 480 nm; emission: 520 nm).[33]

In selected experiments, neutrophils were preincubated with the complement component 5a receptor 1 (C5aR1) antagonist (HY-163379; MedChemExpress) or the toll-like receptor 2 (TLR2) antagonist (HY-116213; MedChemExpress) for 30 min prior to plasma stimulation. Following stimulation, SYTOX Green (5 μM) was added to label extracellular DNA, and NETs formation was assessed immediately by immunofluorescence microscopy.[32]

Immunofluorescence staining

Liver tissue samples were fixed in 4% paraformaldehyde for 24 h at 4 °C, embedded in paraffin, and sectioned at 5 μm thickness.[32] Primary antibodies used were: anti–histone H3 (citrullinated at R2, R8, and R17; Abcam, ab5103), anti-CD31 (Abcam, ab182981), and anti-CD41 (Abcam, ab134131).

ELISA

Plasma concentrations of the following biomarkers were measured using commercially available ELISA kits according to the manufacturers' instructions: NE (RayBiotech, ELH-NEUTRO-1); MPO (NeoBioscience, EHC087.96); syndecan-1 (RayBiotech, ELH-Syndecan1-1); ICAM-1 (RayBiotech, ELH-ICAM1-1); vWF (RayBiotech, ELH-vWF-1); sTM (R&D Systems, DTHBD0); and thrombin–antithrombin complex (TAT; Novus Biologicals, NBP2-68128).

RNA extraction and quantitative real-time PCR

Total RNA was isolated from peripheral blood neutrophils obtained from HC, CHB patients, and HBV-ACLF patients using TRIzol® reagent (Invitrogen, USA), following the manufacturer's instructions. Complementary DNA was synthesized from 1 μg of total RNA using the ReverTra Ace® qPCR RT Master Mix (TOYOBO, Japan), according to the supplier's protocol. Quantitative real-time PCR was performed with SYBR® Green Realtime PCR Master Mix (TOYOBO, Japan) on a CFX96 Touch Real-Time PCR Detection System (Bio-Rad, USA). Primer sequences were as follows: TLR2 forward: 5′-TGCTTTCCTGCTGGAGATTT-3′, reverse: 5′-TGTAACGCAACAGCTTCAGG-3′; C5aR1 forward: 5′-CAGGACATGGACCCCATAGAT-3′, reverse: 5′-ACCAGGAACACCACCGAGTAG-3′; GAPDH forward: 5′-GGAGCGAGATCCCTCCAAAAT-3′, reverse: 5′-GGCTGTTGTCATACTTCTCATGG-3′. All reactions were run in duplicate. Melting curve analysis was conducted after amplification to confirm primer specificity and absence of nonspecific products. Relative mRNA expression levels of TLR2 and C5aR1 were normalized to GAPDH and quantified using the $2^{-\Delta\Delta Ct}$ method.

NETs isolation

Neutrophils (4×10^6 cells/mL) were stimulated with 100 nM phorbol 12-myristate 13-acetate (PMA) for 4 h at 37 °C to induce NETs formation. NETs were isolated using a modified protocol adapted from previously published methods.[34] Briefly, culture medium was removed, and adherent NETs were gently washed twice with 2 mL of ice-cold PBS. The washes were pooled and centrifuged at 1,000 × g for 10 min at 4 °C. The resulting cell-free supernatant containing NETs was collected. The DNA concentration of NETs was measured using a Nanodrop instrument.

Plasma clotting time

Human aortic endothelial cells and HepG2.2.15 cells (an

HBV-infected hepatocyte cell line) were treated with 0.5 ng/mL NETs, DNase 1–digested NETs, or PBS for 6 h.[35] For DNase 1 digestion, NETs were preincubated with 100 U/mL DNase 1 at 37 °C for 30 min. Following treatment, cells were harvested and lysed by three cycles of freezing–thawing followed by sonication. Cell lysates were then assessed for procoagulant activity using a one-stage clotting assay. Specifically, the capacity of each lysate to shorten the spontaneous clotting time of normal citrated human plasma was measured on a coagulation analyzer, and the time to visible fibrin gel formation was recorded.

Statistical analyses

Statistical analyses were conducted using SPSS version 25.0 (IBM Corp., Armonk, NY, USA) and GraphPad Prism (GraphPad Software, San Diego, CA, USA). Categorical variables were summarized as frequencies (percentages) and compared using the chi-square (χ^2) test or Fisher's exact test, as appropriate. Continuous variables were evaluated for normality with the Shapiro–Wilk test. Given that most continuous variables deviated significantly from normality, they were reported as median (IQR).

For comparisons between two independent groups, normally distributed continuous variables were analyzed using the unpaired Student's t-test; non-normally distributed variables were analyzed using the Mann–Whitney U test. For comparisons across three or more independent groups, one-way analysis of variance with Tukey's post hoc test was applied to normally distributed data, whereas the Kruskal–Wallis test followed by Dunn's post hoc test, with Bonferroni correction for multiple comparisons, was used for non-normally distributed data.

Associations between continuous variables were assessed using Spearman's rank correlation coefficient. In linear regression models, influence diagnostics, including Cook's distance and standardized residuals, were performed to identify potentially influential observations. Survival analyses were performed using the Kaplan–Meier method, with between-group differences assessed using the log-rank test. Hazard ratios (HRs) and 95% confidence intervals (CIs) were estimated using Cox proportional hazards regression models. A two-tailed *P*-value < 0.05 was considered statistically significant.

Results

Single-cell transcriptomic profiling reveals neutrophil and LSEC involvement in immunothrombosis in HBV-ACLF liver tissue

In this study, scRNA-seq was performed on non-parenchymal hepatic cells isolated from liver tissues of five patients with HBV-ACLF and four HCs (Fig. 1A). After quality control and batch effect correction (Supplementary Fig. 1A–C), we performed subsequent cell clustering (Fig. 1B) and cell type identification (Fig. 1C and D) using the Seurat software. We then scored multiple coagulation-related pathways, including the complement and coagulation cascades (Kyoto Encyclopedia of Genes and Genomes [KEGG]: hsa04610) and blood coagulation (Gene Ontology: 0007596). These results show that, in addition to the previously reported Kupffer cells,[6] neutrophils and LSEC may also contribute to immunothrombosis in HBV-ACLF (Fig. 1E).

Next, we compared the gene expression profiles of neutrophils and endothelial cells between HBV-ACLF patients and HC, followed by KEGG enrichment analysis. The results demonstrated significant upregulation of pathways related to NETs formation, as well as complement and coagulation activation in neutrophils from HBV-ACLF patients (Fig. 1F). Meanwhile, LSEC from HBV-ACLF patients showed significant upregulation of complement and coagulation activation pathways compared with those from HC (Fig. 1G). These findings indicate that neutrophils and LSEC may be involved in the process of "immunothrombosis" during HBV-ACLF progression.

Circulating NETs are elevated in HBV-ACLF and correlate with coagulopathy and disease severity

To further clarify the role of NETs in immunothrombosis, we enrolled three well-defined patient cohorts: HC, CHB, and HBV-ACLF. A comprehensive comparison of baseline clinical characteristics was conducted across these groups (Table 1). No significant differences in age or gender distribution were observed among the three groups; however, HBV-ACLF patients exhibited significantly higher HBV-DNA levels and more severe liver injury, which was consistent with the expected disease characteristics.

Next, we quantified circulating NETs markers, including MPO–DNA complexes, free MPO, and NE, across the three study groups. Compared with both the CHB and HC groups, patients with HBV-ACLF exhibited significantly elevated levels of all NETs markers (Fig. 2A). Correlation analyses revealed that NETs marker levels were significantly associated with key coagulation parameters, including the INR and thrombin-antithrombin complex (TAT) (Fig. 2B), as well as prothrombin time, PTA, and activated partial thromboplastin time (APTT) (Supplementary Fig. 2A). Furthermore, NETs levels correlated positively with serum lactate dehydrogenase (LDH) (Fig. 2C), a well-established biomarker of cellular injury,[36] as well as with serum cholinesterase and the neutrophil-to-lymphocyte ratio (Supplementary Fig. 2B and C). Significant positive correlations were also observed between NETs levels and established prognostic scoring systems, specifically the MELD-Na and the Chinese Group on the Study of Severe Hepatitis B–ACLF II (COSSH-ACLF II) scores (Fig. 2D).

Notably, circulating NETs levels were significantly higher in non-survivors than in survivors (Fig. 2E). Kaplan–Meier survival analysis further demonstrated that elevated NETs levels were associated with significantly increased 90-day mortality (log-rank test, $P < 0.01$; HR = 3.92; 95% CI: 1.94–7.94) (Fig. 2F). Clinical characteristics distinguishing survivors and non-survivors were summarized in Supplementary Table 1. Collectively, these findings indicate that NETs formation is closely linked to coagulopathy, hepatocellular injury, and adverse clinical outcomes in HBV-ACLF.

Endothelial injury is markedly aggravated in HBV-ACLF and closely associated with disease severity

To assess endothelial dysfunction and concomitant coagulation activation,[37–39] we quantified circulating levels of four established biomarkers: syndecan-1, vWF, sTM, and ICAM-1. All four markers were significantly elevated in HBV-ACLF patients relative to both CHB patients and HC (Fig. 3A–C). Stratified analyses further revealed that non-survivors exhibited significantly higher circulating levels of syndecan-1, vWF, and ICAM-1 compared with survivors (Fig. 3D–F). Notably, syndecan-1 levels demonstrated strong positive correlations with the TAT, INR, and MELD-Na score (Fig. 3G and H), as well as with LDH and serum creatinine (Supplementary Fig. 3A and B). Consistently, correlation heatmap analysis demonstrated significant associations between endothelial-related markers and indices of disease severity and prognosis (Fig. 3I). Together, these findings indicate that endothelial

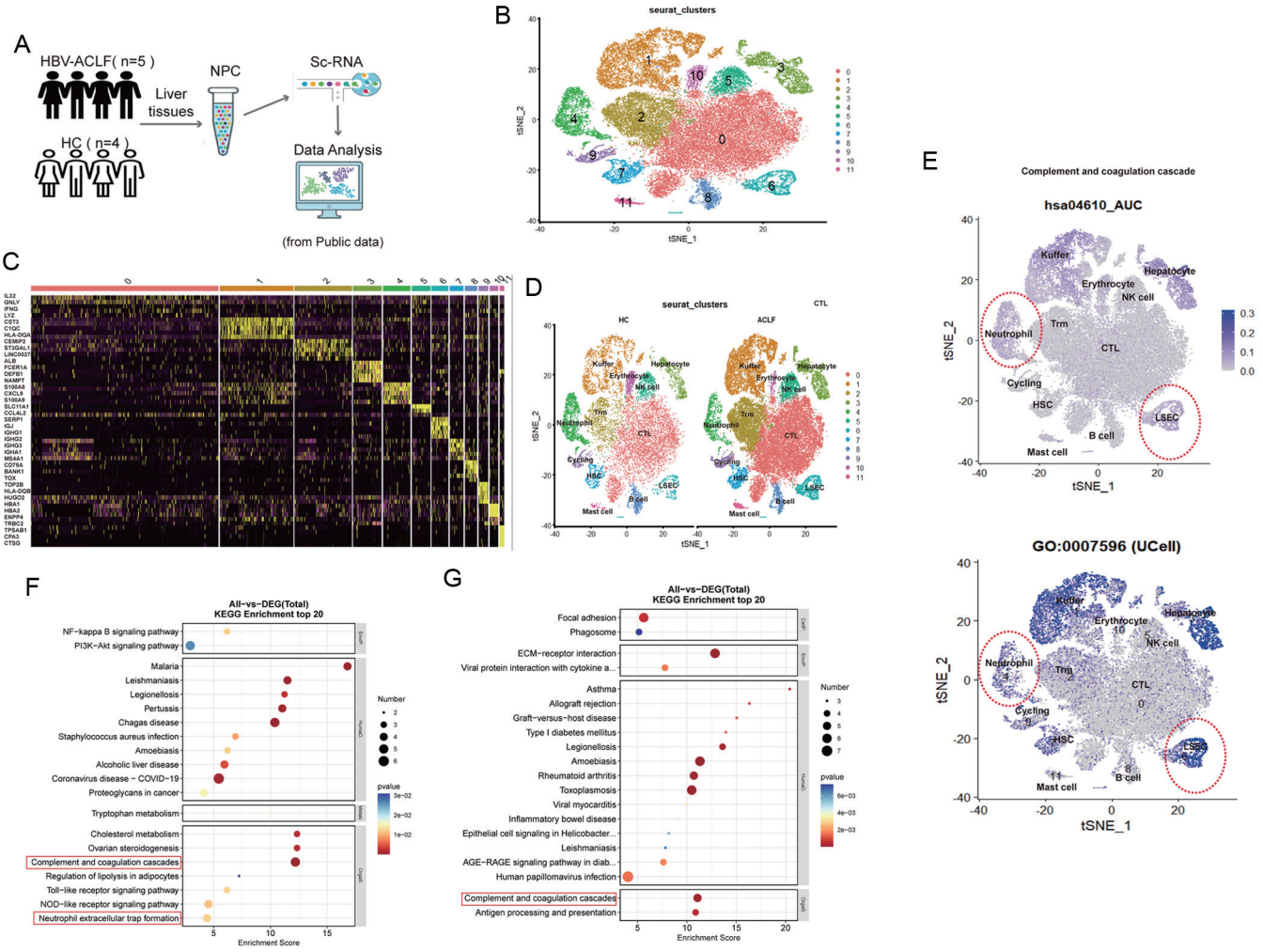

Fig. 1. Coagulation-related pathway scores in neutrophils and LSEC from liver samples of patients with HBV-ACLF. (A) Workflow of scRNA-seq analysis. (B) t-SNE plot of non-parenchymal liver cells showing 12 cell clusters. (C) Heatmap of differentially expressed genes across the 12 subclusters. (D) Cell-type annotation based on canonical marker gene expression in HBV-ACLF patients and HC. (E) UCell scoring and visualization of two coagulation-related pathways: the complement and coagulation cascades (KEGG: hsa04610) and blood coagulation (GO: 0007596). (F–G) KEGG enrichment analysis performed on differentially expressed genes in neutrophils (F) and LSEC (G) from HBV-ACLF patients and HC. LSEC, liver sinusoidal endothelial cells; HBV-ACLF, hepatitis B virus-related acute-on-chronic liver failure; scRNA-seq, single-cell RNA sequencing; HC, healthy controls; KEGG, Kyoto Encyclopedia of Genes and Genomes; GO, Gene Ontology.

dysfunction is closely linked to coagulation activation, organ injury, and adverse clinical outcomes in HBV-ACLF.

NETs are associated with endothelial injury and coagulation dysfunction in HBV-ACLF

Given the established role of NETs in endothelial activation, we investigated their association with established biomarkers of endothelial injury. NETs levels exhibited significant positive correlations with syndecan-1, ICAM-1, sTM, and vWF, as shown in Figure 4A–C. Immunofluorescence staining of liver tissues revealed abundant NETs formation in patients with HBV-ACLF; notably, these NETs colocalized with CD31-positive endothelial cells and CD41-positive platelets within microthrombi (Fig. 4D). *In vitro* experiments demonstrated that NETs isolated from neutrophils of HBV-infected individuals significantly elevated syndecan-1 levels and shortened plasma clotting time, a procoagulant effect that was markedly attenuated by DNase I treatment (Fig. 4E). Similarly, NETs enhanced the procoagulant activity of HBV-infected hepatocytes (HepG2.2.15 cells), and this effect was reversed by DNase I treatment (Fig. 4F). Collectively, these findings indicate that NETs are associated with endothelial injury and a prothrombotic milieu in HBV-ACLF.

TLR2 and C5aR1 signaling are involved in NETs formation within the HBV-ACLF plasma microenvironment

NETs formation can be induced by both microbial and endogenous stimuli, including damage-associated molecular patterns (DAMPs) and complement activation products.[40] To delineate the upstream signaling pathways driving NETs formation in HBV-ACLF, we performed integrated omics analyses comparing neutrophils from HBV-ACLF patients and HC. These analyses identified C5aR1 and TLR2 as potential mediators of this process (Fig. 5A). Consistently, peripheral blood neutrophils isolated from HBV-ACLF patients exhibited significantly higher expression levels of both TLR2 and C5aR1 compared with those from HC (Fig. 5B). Functional assays further demonstrated that plasma from HBV-ACLF patients

Table 1. Baseline characteristics

Characteristic	Healthy controls (n = 20)	CHB (n = 20)	ACLF (n = 46)	*P*-value
Age (years)	46 (33–56)	40 (32–50)	46 (33–56)	0.08
Male, n (%)	90% (18)	85% (17)	91.3% (42)	0.78
Cirrhosis, n (%)	–	40% (8)	56.5% (26)	0.29
HBV DNA level (Copy/mL)	–	258.9 (20–4,387.5)	67,550 (1,167.5–3,710,000)	<0.01
Infection	–	–	23.91% (11)	–
Artificial liver support	–	–	26.09% (12)	–
Anticoagulation/antiplatelet	–	–	0% (0)	–
Laboratory data				
Alanine aminotransferase (U/L)	19.5 (12.5–23)	22.5 (10.3–34)	213 (78.8–473.3)	<0.01
Aspartate aminotransferase (U/L)	19 (17.3–23.8)	23 (14.5–27)	109 (77–386.8)	<0.01
Alkaline phosphatase (U/L)	68.5 (53–77)	69.5 (62.3–77.3)	134.5 (114.5–155.5)	<0.01
Albumin (g/L)	46.4 (45.9–48.1)	46.7 (45.1–48.4)	32.5 (29.6–36.4)	<0.01
Total bilirubin (μmol/L)	14.0 (10.4–16.9)	10.5 (7.7–15.7)	339.6 (251.2–460.5)	<0.01
Creatinine (μmol/L)	–	–	66 (56–82)	–
White blood cell count (10^9/L)	–	–	4.19 (3.5325–6.61)	–
Hemoglobin (g/L)	–	–	120.5 (105.25–133.25)	–
Platelet count (10^9/L)	–	–	102 (57.75–131.5)	–
INR	–	–	2.16 (1.69–2.88)	–
Severity score				–
COSSH-ACLF II	–	–	6.9 (6.0 –7.8)	–
MELD	–	–	24.1 (20.1–29.7)	–
MELD-Na	–	–	26.7 (22.5–33.4)	–

Continuous variables are presented as median (interquartile range), and categorical variables as percentages (with absolute counts). ACLF, acute-on-chronic liver failure; CHB, chronic hepatitis B; INR, international normalized ratio; MELD, Model for End-Stage Liver Disease; MELD-Na, MELD-sodium; COSSH-ACLF II, Chinese Onset Study of Severe Hepatitis with Acute-on-Chronic Liver Failure II.

induced markedly greater NETs release in neutrophils isolated from healthy donors than plasma from HC (Fig. 5C and D). Importantly, pharmacological inhibition of either TLR2 or C5aR1 significantly attenuated NETs formation induced by HBV-ACLF plasma, indicating that the pro-NETosis plasma microenvironment in HBV-ACLF acted through TLR2- and C5aR1-dependent signaling pathways (Fig. 5E).

Discussion

The pathogenic role of NETs in ACLF has garnered increasing attention; however, findings from mixed-etiology cohorts remain inconsistent, largely attributable to substantial mechanistic heterogeneity across underlying etiologies.[41–44] In contrast, studies focusing on HBV-ACLF have more consistently reported elevated circulating NETs components and their association with disease severity and clinical outcomes.[32,45,46] In line with these observations, our findings are consistent with the clinical relevance of NETs in HBV-ACLF. Importantly, by integrating endothelial injury markers and coagulation parameters, this work extends prior studies and suggests a potential association between NETs, endothelial dysfunction, and coagulopathy in this setting.

Previous studies have suggested that neutrophils may adopt a primed phenotype under inflammatory conditions,[40] and endothelial cells may exhibit procoagulant features in the setting of severe liver injury.[18] In line with these concepts, single-cell transcriptomic data are consistent with coordinated transcriptional features in neutrophils and LSEC aligned with NETs-related and coagulation-associated pathways. Together with prior observations of spatial associations between NETs components, endothelial cells, and platelets,[39,47,48] these findings extend existing knowledge by suggesting that such interactions in HBV-ACLF may exhibit a liver-restricted distribution, potentially reflecting organ-specific organization of immunothrombosis.

Although prior studies have indicated that NETs contribute to endothelial dysfunction and promote coagulation activation in inflammatory disease,[37,49] whether NETs function as active drivers versus bystanders in disease progression remains unclear in HBV-ACLF. In this context, the present findings extend these observations by providing evidence that NETs may be linked to endothelial perturbation and procoagulant activity in a disease-specific setting. In addition, TLR2 and C5aR1 signaling pathways, previously implicated in NETs induction,[50,51] may also participate in this process in HBV-ACLF, suggesting a context-dependent involvement of these pathways within a liver-centered immunothrombotic framework.

Although NETs-mediated immunothrombosis has been extensively characterized in sepsis, disease-specific differences in triggering mechanisms and spatial distribution are

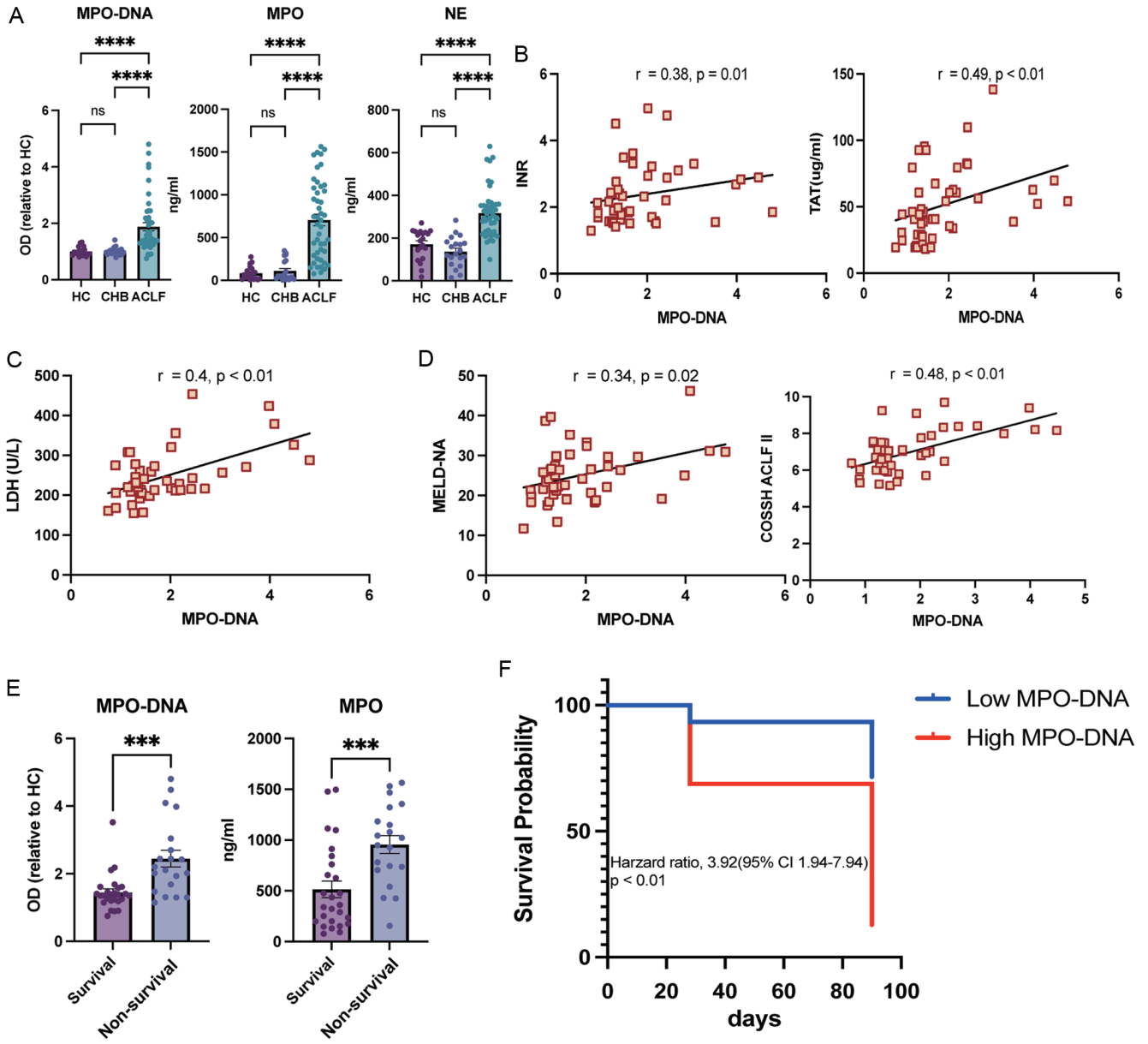

Fig. 2. Plasma NETs markers and clinical parameters in patients with HBV-ACLF. (A) Plasma concentrations of NETs markers, including MPO–DNA complexes, MPO, and NE, in HBV-ACLF, CHB, and HC groups. (B–C) Correlations between plasma MPO–DNA levels and INR and TAT (B), and LDH (C). (D) Correlations between plasma MPO–DNA levels and established prognostic scoring systems, including the COSSH-ACLF II and MELD-Na scores. (E) Comparison of NETs marker levels (MPO–DNA and MPO) between survivors and non-survivors within the HBV-ACLF cohort. (F) Kaplan–Meier survival curves of HBV-ACLF patients stratified by plasma MPO–DNA levels (≤2-fold vs >2-fold). $^{***}P < 0.001$, and $^{****}P < 0.0001$. NETs, neutrophil extracellular traps; HBV-ACLF, hepatitis B virus-related acute-on-chronic liver failure; MPO, myeloperoxidase; NE, neutrophil elastase; CHB, chronic hepatitis B; HC, healthy controls; INR, international normalized ratio; TAT, thrombin-antithrombin complex; LDH, lactate dehydrogenase; COSSH-ACLF II, Chinese Onset Study of Severe Hepatitis with Acute-on-Chronic Liver Failure II; MELD-Na, Model for End-Stage Liver Disease-Sodium.

increasingly recognized. In sepsis, NETs formation is typically driven by pathogen-associated stimuli and is associated with systemic microvascular thrombosis and remote organ injury.[14,47] In contrast, HBV-ACLF is characterized by extensive hepatocellular necrosis and the release of DAMPs, which are thought to be major drivers of inflammatory activation.[22,46] In this setting, NETs deposition appears to be more restricted to hepatic sinusoids and associated with local endothelial injury and microcirculatory dysfunction. These distinctions suggest that, in contrast to the predominantly systemic nature of immunothrombosis in sepsis, HBV-ACLF may exhibit a more liver-centered and spatially restricted pattern. This context-specific organization may provide a potential mechanistic framework linking parenchymal injury with intrahepatic coagulation dysregulation.

Based on these multi-level observations, a conceptual framework can be proposed in which hepatocellular injury may initiate NETs formation through DAMP release,[40] while excessive NETs may contribute to endothelial dysfunction and coagulation activation.[14,37] This integrative model may

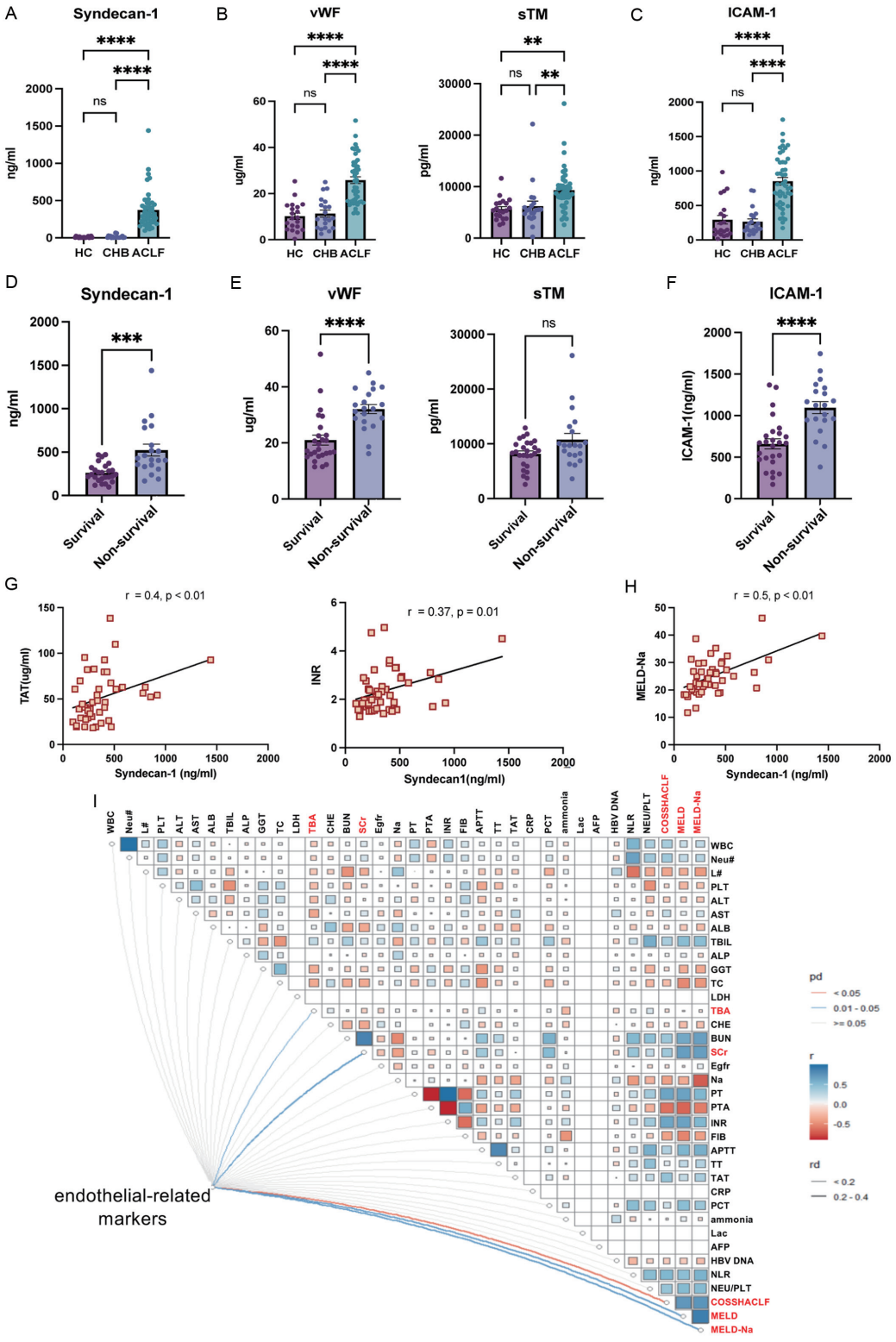

Fig. 3. Plasma endothelial injury biomarkers in patients with HBV-ACLF. (A–C) Plasma concentrations of syndecan-1 (A), vWF and sTM (B), and ICAM-1 (C) in HBV-ACLF, CHB, and HC. (D–F) Comparison of plasma syndecan-1 (D), vWF and sTM (E), and ICAM-1 (F) levels between survivors and non-survivors within the HBV-ACLF cohort. (G–H) Correlation analyses of plasma syndecan-1 levels with TAT and INR (G), and with the MELD-Na score (H). (I) Heatmap of pairwise correlations between a composite endothelial injury biomarker panel and clinical parameters. $^{**}P < 0.01$, $^{***}P < 0.001$, and $^{****}P < 0.0001$. HBV-ACLF, hepatitis B virus-related acute-on-chronic liver failure; vWF, von Willebrand factor; sTM, soluble thrombomodulin; ICAM-1, intercellular adhesion molecule-1; CHB, chronic hepatitis B; HC, healthy controls; TAT, thrombin-antithrombin complex; INR, international normalized ratio; MELD-Na, Model for End-Stage Liver Disease-Sodium.

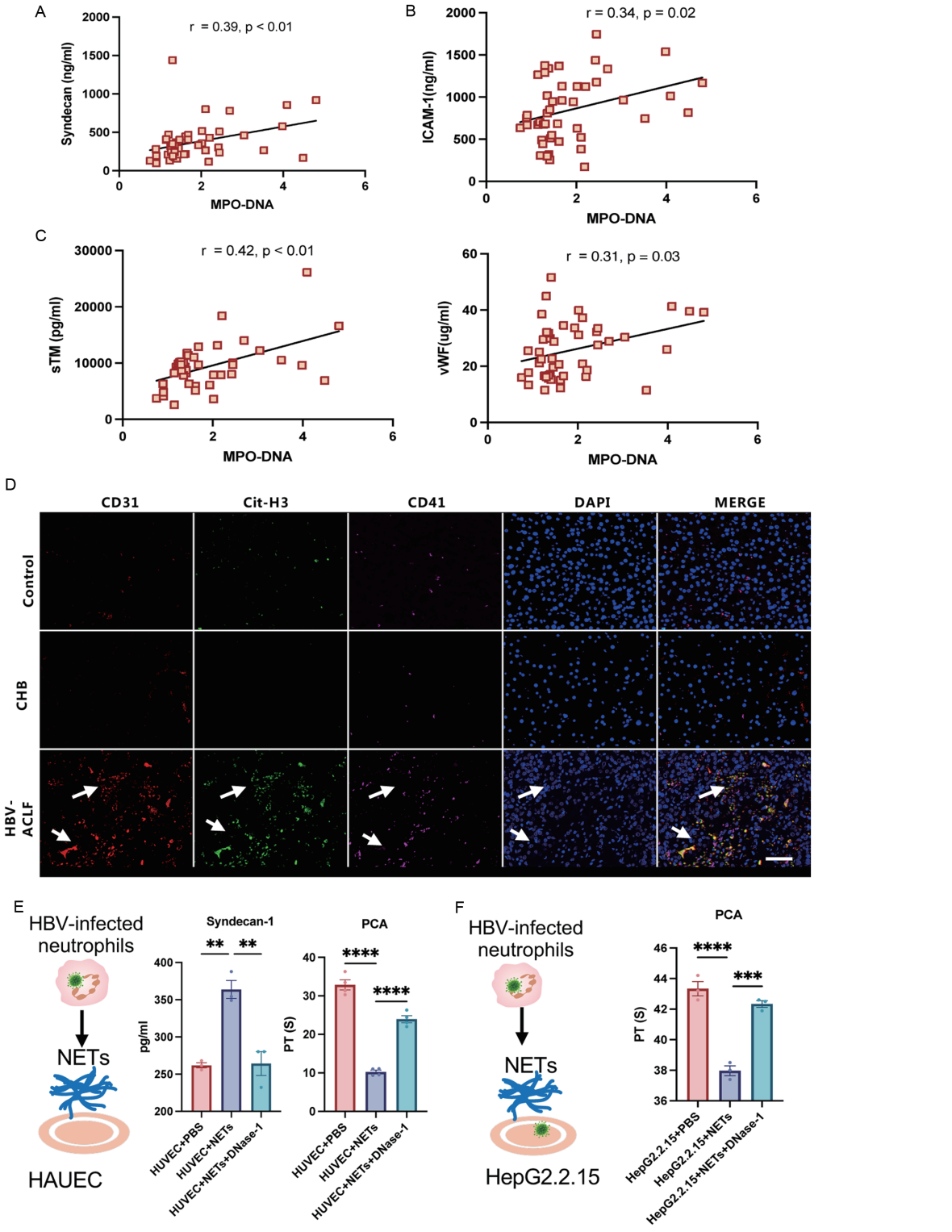

Fig. 4. NETs markers, endothelial injury biomarkers, and coagulation parameters in HBV-ACLF. (A–C) Correlation analyses between plasma MPO–DNA complex levels and syndecan-1 (A), ICAM-1 (B), and sTM and vWF (C). (D) Immunofluorescence staining of endothelial cells (CD31), NETs (citrullinated histone H3, Cit-H3), and platelets (CD41) in liver tissues from patients with HBV-ACLF, CHB, and HC. Scale bars: 50 μm. (E) Neutrophils isolated from CHB patients were stimulated with PMA. NETs were collected and incubated with human aortic endothelial cells, with or without DNase I treatment. Syndecan-1 levels in supernatants and plasma clotting time of cells were measured after 6 h. $^{**}P < 0.01$, $^{***}P < 0.001$, and $^{****}P < 0.0001$. NETs, neutrophil extracellular traps; HBV-ACLF, hepatitis B virus-related acute-on-chronic liver failure; MPO, myeloperoxidase; ICAM-1, intercellular adhesion molecule-1; sTM, soluble thrombomodulin; vWF, von Willebrand factor; CHB, chronic hepatitis B; HC, healthy controls; PMA, phorbol 12-myristate 13-acetate; DNase I, deoxyribonuclease I.

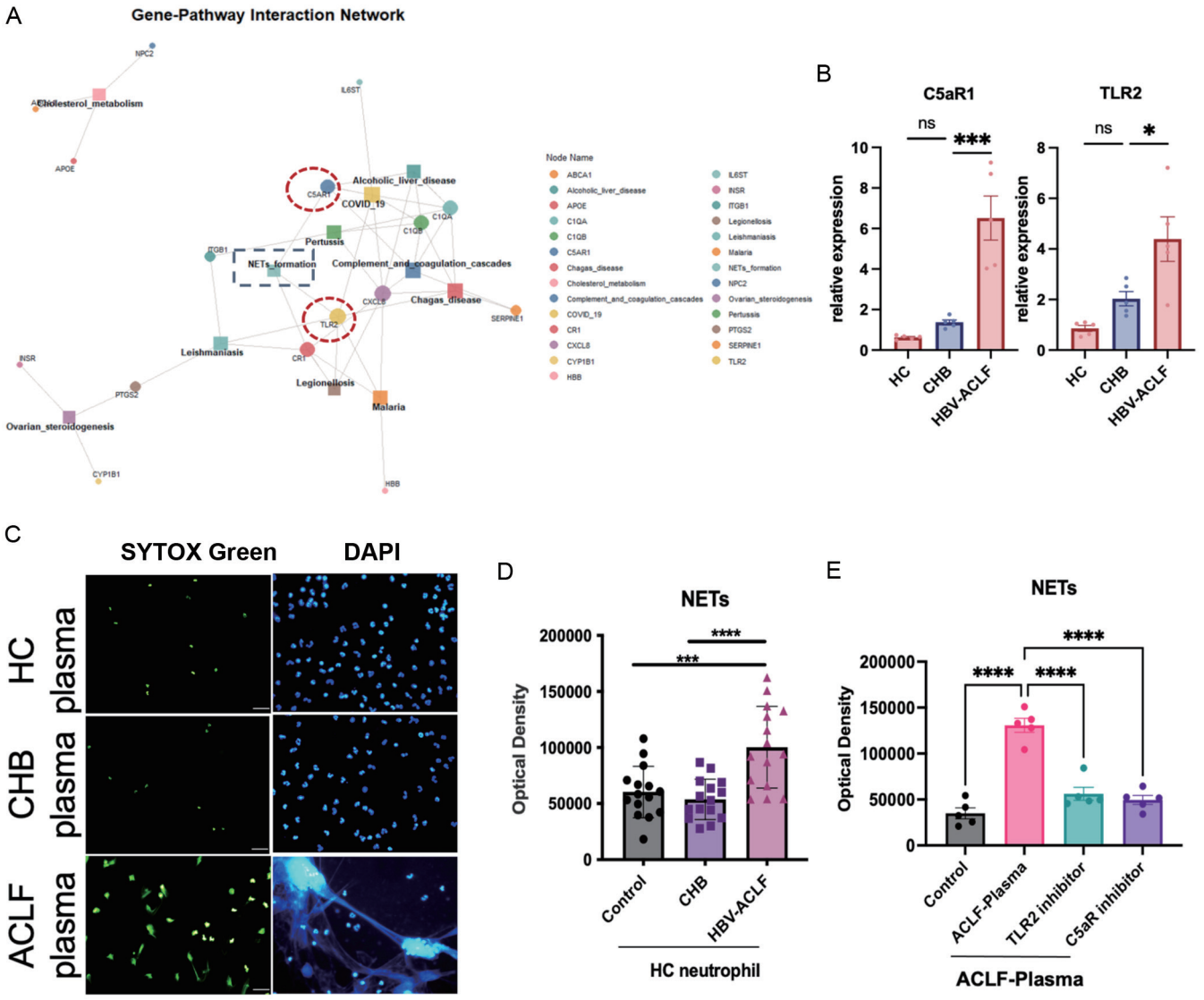

Fig. 5. NETs formation in neutrophils stimulated with HBV-ACLF plasma in the presence of TLR2 or C5aR1 inhibitors. (A) Visualization of differentially expressed genes and pathways in neutrophils from HBV-ACLF patients and HC using the circlize R package. (B) mRNA expression levels of TLR2 and C5aR1 in neutrophils from HC, CHB, and HBV-ACLF patients. (C) Immunofluorescence images (SYTOX Green and DAPI) in neutrophils stimulated with plasma from HC, CHB, and HBV-ACLF groups. Scale bars: 50 μm. (D) Quantification of NETs release from neutrophils stimulated with plasma from HC, CHB, and HBV-ACLF groups, measured by SYTOX Green fluorescence. (E) NETs release in the presence or absence of TLR2 or C5aR1 inhibitors. $^{*}P < 0.05$, $^{***}P < 0.001$, and $^{****}P < 0.0001$. NETs, neutrophil extracellular traps; HBV-ACLF, hepatitis B virus-related acute-on-chronic liver failure; TLR2, toll-like receptor 2; C5aR1, complement component 5a receptor 1; CHB, chronic hepatitis B; HC, healthy controls.

extend existing paradigms by linking immune activation, vascular injury, and coagulation into a unified, liver-centered process in HBV-ACLF.

These findings may also have therapeutic implications. Previous studies have explored NETs-targeted interventions in liver disease.[10,32] In this context, strategies aimed at modulating the NETs–endothelial–coagulation axis, including enhancing NETs degradation or targeting upstream signaling pathways, may represent potential approaches, although their efficacy and safety require further evaluation in physiologically relevant models.

Several limitations should be acknowledged. Firstly, the sample size may limit statistical power for subgroup analyses and adjustment for potential confounders. Secondly, the observational design of the clinical component inherently limits its causal inference. Thirdly, while *in vitro* experiments offer valuable mechanistic insights, they cannot fully recapitulate the intricate hepatic microenvironment characteristic of HBV-ACLF. Future studies should include longitudinal analyses to assess whether NETs dynamics are associated with disease progression and clinical outcomes, as well as interventional studies in relevant animal models. Independent validation in larger, multicenter cohorts will also be important to strengthen generalizability.

Conclusions

Our study provides multi-level evidence linking NETs formation with endothelial injury and immunothrombosis in HBV-ACLF. By integrating clinical, spatial, transcriptomic,

and functional data, we outline a liver-centered framework in which NETs may be associated with intrahepatic coagulation disturbances. Although causality remains to be established, NETs and their upstream pathways, including TLR2 and C5aR1, may represent potential targets for future therapeutic investigation in HBV-ACLF.

Funding

This work was supported by the National Key Research and Development Program of China (2023YFC2308600), the National Natural Science Foundation of China (No. 82370609, No. 82170596), the National Youth Talent Support Program (No. 0106540082), and the Hubei Province Science and Technology Development Special Fund (2024CSA064).

Conflict of interest

QN has been an Editorial Board Member of *Journal of Clinical and Translational Hepatology* since 2024. The other authors have no conflict of interests related to this publication.

Author contributions

Project design (QN, XW, XL), clinical data collection (XL, SH), experiment performance (XL, SH), assistance for experiment performance (XZ, PH), data discussion, providing suggestions (WW, QG, JH, BY, FX, HX), data analysis (XL), assistance for data analysis (PH, XZ), writing of the manuscript (XL), and revision of the manuscript (QN, XW). All authors have approved the final version and publication of the manuscript.

Ethical statement

This study was reviewed and approved by the local ethics committee of Tongji Hospital, Tongji Medical College, Huazhong University of Science and Technology (2021S125), and was conducted in accordance with the Declaration of Helsinki (as revised in 2024). All patients signed written informed consent for tissue analysis prior to the procedure.

Data sharing statement

All data generated or analyzed in this study are available from the corresponding author upon reasonable request.

References

[1] Hernaez R, Solà E, Moreau R, Ginès P. Acute-on-chronic liver failure: an update. Gut 2017;66(3):541–553. doi:10.1136/gutjnl-2016-312670, PMID:28053053.
[2] Zhang Y, Tan W, Wang X, Zheng X, Huang Y, Li B, *et al*. Investigation on the short-term outcome and prognostic impact of predisposition, and precipitants in inpatients with chronic liver disease from Chinese Acute On Chronic Liver Failure (CATCH-LIFE) cohorts. Portal Hypertens Cirrhosis 2023;2(3):115–126. doi:10.1002/poh2.53.
[3] Abbas N, Rajoriya N, Elsharkawy AM, Chauhan A. Acute-on-chronic liver failure (ACLF) in 2022: have novel treatment paradigms already arrived? Expert Rev Gastroenterol Hepatol 2022;16(7):639–652. doi:10.1080/17474124.2022.2097070, PMID:35786130.
[4] Li J, Liang X, Jiang J, Yang L, Xin J, Shi D, *et al*. PBMC transcriptomics identifies immune-metabolism disorder during the development of HBV-ACLF. Gut 2022;71(1):163–175. doi:10.1136/gutjnl-2020-323395, PMID:33431576.
[5] Engelmann B, Massberg S. Thrombosis as an intravascular effector of innate immunity. Nat Rev Immunol 2013;13(1):34–45. doi:10.1038/nri3345, PMID:23222502.
[6] Marsden PA, Ning Q, Fung LS, Luo X, Chen Y, Mendicino M, *et al*. The Fgl2/fibroleukin prothrombinase contributes to immunologically mediated thrombosis in experimental and human viral hepatitis. J Clin Invest 2003;112(1):58–66. doi:10.1172/JCI18114, PMID:12840059.
[7] Yu M, Li X, Xu L, Zheng C, Pan W, Chen H, *et al*. Neutrophil extracellular traps induce intrahepatic thrombotic tendency and liver damage in cholestatic liver disease. Hepatol Commun 2024;8(8):e0513. doi:10.1097/HC9.0000000000000513, PMID:39101776.
[8] Chen Z, Zhang H, Qu M, Nan K, Cao H, Cata JP, *et al*. Review: The Emerging Role of Neutrophil Extracellular Traps in Sepsis and Sepsis-Associated Thrombosis. Front Cell Infect Microbiol 2021;11:653228. doi:10.3389/fcimb.2021.653228, PMID:33816356.
[9] Middleton EA, He XY, Denorme F, Campbell RA, Ng D, Salvatore SP, *et al*. Neutrophil extracellular traps contribute to immunothrombosis in COVID-19 acute respiratory distress syndrome. Blood 2020;136(10):1169–1179. doi:10.1182/blood.2020007008, PMID:32597954.
[10] Lee YY, Park HH, Park W, Kim H, Jang JG, Hong KS, *et al*. Long-acting nanoparticulate DNase-1 for effective suppression of SARS-CoV-2-mediated neutrophil activities and cytokine storm. Biomaterials 2021;267:120389. doi:10.1016/j.biomaterials.2020.120389, PMID:33130319.
[11] Adrover JM, Carrau L, Daßler-Plenker J, Bram Y, Chandar V, Houghton S, *et al*. Disulfiram inhibits neutrophil extracellular trap formation and protects rodents from acute lung injury and SARS-CoV-2 infection. JCI Insight 2022;7(5):e157342. doi:10.1172/jci.insight.157342, PMID:35133984.
[12] Liang X, Luo J, Zhou Q, Xin J, Li J, Peng B, *et al*. Single-cell multimodal analysis reveals the dynamic immunopathogenesis of HBV-ACLF progression. Gut 2026;75(2):367–381. doi:10.1136/gutjnl-2024-333308, PMID:40841166.
[13] Wu T, Li J, Shao L, Xin J, Jiang L, Zhou Q, *et al*. Development of diagnostic criteria and a prognostic score for hepatitis B virus-related acute-on-chronic liver failure. Gut 2018;67(12):2181–2191. doi:10.1136/gutjnl-2017-314641, PMID:28928275.
[14] Zhang H, Wang Y, Qu M, Li W, Wu D, Cata JP, *et al*. Neutrophil, neutrophil extracellular traps and endothelial cell dysfunction in sepsis. Clin Transl Med 2023;13(1):e1170. doi:10.1002/ctm2.1170, PMID:36629024.
[15] Rangaswamy C, Englert H, Deppermann C, Renné T. Polyanions in Coagulation and Thrombosis: Focus on Polyphosphate and Neutrophils Extracellular Traps. Thromb Haemost 2021;121(8):1021–1030. doi:10.1055/a-1336-0526, PMID:33307564.
[16] Fuchs TA, Brill A, Duerschmied D, Schatzberg D, Monestier M, Myers DD Jr, *et al*. Extracellular DNA traps promote thrombosis. Proc Natl Acad Sci U S A 2010;107(36):15880–15885. doi:10.1073/pnas.1005743107, PMID:20798043.
[17] Bautista-Becerril B, Campi-Caballero R, Sevilla-Fuentes S, Hernández-Regino LM, Hanono A, Flores-Bustamante A, *et al*. Immunothrombosis in COVID-19: Implications of Neutrophil Extracellular Traps. Biomolecules 2021;11(5):694. doi:10.3390/biom11050694, PMID:34066385.
[18] Gracia-Sancho J, Caparrós E, Fernández-Iglesias A, Francés R. Role of liver sinusoidal endothelial cells in liver diseases. Nat Rev Gastroenterol Hepatol 2021;18(6):411–431. doi:10.1038/s41575-020-00411-3, PMID:33589830.
[19] Zhou X, Luo J, Liang X, Li P, Ren K, Shi D, *et al*. Plasma thrombomodulin as a candidate biomarker for the diagnosis and prognosis of HBV-related acute-on-chronic liver failure. Infect Drug Resist 2024;17:1185–1198. doi:10.2147/IDR.S437926, PMID:38560706.
[20] Zhang P, Li H, Zhou C, Liu K, Peng B, She X, *et al*. Single-Cell RNA Transcriptomics Reveals the State of Hepatic Lymphatic Endothelial Cells in Hepatitis B Virus-Related Acute-on-Chronic Liver Failure. J Clin Med 2022;11(10):2910. doi:10.3390/jcm11102910, PMID:35629036.
[21] Zhang M, Kong Y, Xu X, Sun Y, Jia J, You H. "Treat-all" Strategy for Patients with Chronic Hepatitis B Virus Infection in China: Are We There Yet? J Clin Transl Hepatol 2024;12(6):589–593. doi:10.14218/JCTH.2024.00091, PMID:38974957.
[22] Br VK, Sarin SK. Acute-on-chronic liver failure: Terminology, mechanisms and management. Clin Mol Hepatol 2023;29(3):670–689. doi:10.3350/cmh.2022.0103, PMID:36938601.
[23] Choudhury A, Kulkarni AV, Arora V, Soin AS, Dokmeci AK, Chowdhury A, *et al*. Acute-on-chronic liver failure (ACLF): the 'Kyoto Consensus'-steps from Asia. Hepatol Int 2025;19(1):1–69. doi:10.1007/s12072-024-10773-4, PMID:39961976.
[24] Li J, Liang X, You S, Feng T, Zhou X, Zhu B, *et al*. Development and validation of a new prognostic score for hepatitis B virus-related acute-on-chronic liver failure. J Hepatol 2021;75(5):1104–1115. doi:10.1016/j.jhep.2021.05.026, PMID:34090929.
[25] Malinchoc M, Kamath PS, Gordon FD, Peine CJ, Rank J, ter Borg PC. A model to predict poor survival in patients undergoing transjugular intrahepatic portosystemic shunts. Hepatology 2000;31(4):864–871. doi:10.1053/he.2000.5852, PMID:10733541.
[26] Biggins SW, Kim WR, Terrault NA, Saab S, Balan V, Schiano T, *et al*. Evidence-based incorporation of serum sodium concentration into MELD. Gastroenterology 2006;130(6):1652–1660. doi:10.1053/j.gastro.2006.02.010, PMID:16697729.
[27] Zheng GX, Terry JM, Belgrader P, Ryvkin P, Bent ZW, Wilson R, *et al*. Massively parallel digital transcriptional profiling of single cells. Nat Commun 2017;8:14049. doi:10.1038/ncomms14049, PMID:28091601.
[28] Hao Y, Hao S, Andersen-Nissen E, Mauck WM 3rd, Zheng S, Butler A, *et al*. Integrated analysis of multimodal single-cell data. Cell 2021;184(13):3573–3587.e29. doi:10.1016/j.cell.2021.04.048, PMID:34062119.
[29] Hafemeister C, Satija R. Normalization and variance stabilization of single-cell RNA-seq data using regularized negative binomial regression. Genome Biol 2019;20(1):296. doi:10.1186/s13059-019-1874-1, PMID:31870423.
[30] Becht E, McInnes L, Healy J, Dutertre CA, Kwok IWH, Ng LG, *et al*. Dimensionality reduction for visualizing single-cell data using UMAP. Nat Biotechnol 2019;37:38–44. doi:10.1038/nbt.4314, PMID:30531897.
[31] Zhan X, Wu R, Kong XH, You Y, He K, Sun XY, *et al*. Elevated neutrophil extracellular traps by HBV-mediated S100A9-TLR4/RAGE-ROS cas-

cade facilitate the growth and metastasis of hepatocellular carcinoma. Cancer Commun (Lond) 2023;43(2):225–245. doi:10.1002/cac2.12388, PMID:36346061.
[32] Li X, Gao Q, Wu W, Hai S, Hu J, You J, *et al*. FGL2-MCOLN3-Autophagy Axis-Triggered Neutrophil Extracellular Traps Exacerbate Liver Injury in Fulminant Viral Hepatitis. Cell Mol Gastroenterol Hepatol 2022;14(5):1077–1101. doi:10.1016/j.jcmgh.2022.07.014, PMID:35926777.
[33] Vong L, Sherman PM, Glogauer M. Quantification and Visualization of Neutrophil Extracellular Traps (NETs) from Murine Bone Marrow-Derived Neutrophils. Methods Mol Biol 2019;1960:63–73. doi:10.1007/978-1-4939-9167-9_5, PMID:30798521.
[34] Yang L, Liu Q, Zhang X, Liu X, Zhou B, Chen J, *et al*. DNA of neutrophil extracellular traps promotes cancer metastasis via CCDC25. Nature 2020;583(7814):133–138. doi:10.1038/s41586-020-2394-6, PMID:32528174.
[35] Ngo AT, Skidmore A, Oberg J, Yarovoi I, Sarkar A, Levine N, *et al*. Platelet factor 4 limits neutrophil extracellular trap- and cell-free DNA-induced thrombogenicity and endothelial injury. JCI Insight 2023;8(22):e171054. doi:10.1172/jci.insight.171054, PMID:37991024.
[36] Price JR, Hagrass H, Filip AB, McGill MR. LDH and the MELD-LDH in Severe Acute Liver Injury and Acute Liver Failure: Preliminary Confirmation of a Novel Prognostic Score for Risk Stratification. J Appl Lab Med 2023;8(3):504–513. doi:10.1093/jalm/jfac137, PMID:36759930.
[37] Maneta E, Aivalioti E, Tual-Chalot S, Emini Veseli B, Gatsiou A, Stamatelopoulos K, *et al*. Endothelial dysfunction and immunothrombosis in sepsis. Front Immunol 2023;14:1144229. doi:10.3389/fimmu.2023.1144229, PMID:37081895.
[38] Joffre J, Hellman J, Ince C, Ait-Oufella H. Endothelial Responses in Sepsis. Am J Respir Crit Care Med 2020;202(3):361–370. doi:10.1164/rccm.201910-1911TR, PMID:32101446.
[39] Folco EJ, Mawson TL, Vromman A, Bernardes-Souza B, Franck G, Persson O, *et al*. Neutrophil Extracellular Traps Induce Endothelial Cell Activation and Tissue Factor Production Through Interleukin-1α and Cathepsin G. Arterioscler Thromb Vasc Biol 2018;38(8):1901–1912. doi:10.1161/ATVBAHA.118.311150, PMID:29976772.
[40] Papayannopoulos V. Neutrophil extracellular traps in immunity and disease. Nat Rev Immunol 2018;18(2):134–147. doi:10.1038/nri.2017.105, PMID:28990587.
[41] Zhang Y, Shi K, Zhu B, Feng Y, Liu Y, Wang X. Neutrophil Extracellular Trap Scores Predict 90-Day Mortality in Hepatitis B-Related Acute-on-Chronic Liver Failure. Biomedicines 2024;12(9):2048. doi:10.3390/biomedicines12092048, PMID:39335563.
[42] Balcar L, Scheiner B, Simbrunner B, Jachs M, Hartl L, Semmler G, *et al*. Neutrophil Extracellular Traps Are Not Linked to Decompensation, ACLF, or Death in Clinically Stable Patients With ACLD. Liver Int 2025;45(10):e70323. doi:10.1111/liv.70323, PMID:40965468.
[43] Blasi A, Patel VC, Adelmeijer J, Azarian S, Aziz F, Fernández J, *et al*. Plasma levels of circulating DNA are associated with outcome, but not with activation of coagulation in decompensated cirrhosis and ACLF. JHEP Rep 2019;1(3):179–187. doi:10.1016/j.jhepr.2019.06.002, PMID:32039368.
[44] Ortega-Ribera M, Zhuang Y, Babuta M, Brezani V, Joshi RS, Zsengeller Z, *et al*. A Novel Multi-organ Male Model of Alcohol-induced Acute-on-chronic Liver Failure Reveals NET-mediated Hepatocellular Death, Which is Prevented by RIPK3 Inhibition. Cell Mol Gastroenterol Hepatol 2025;19(4):101446. doi:10.1016/j.jcmgh.2024.101446, PMID:39710168.
[45] Wu W, Sun S, Wang Y, Zhao R, Ren H, Li Z, *et al*. Circulating Neutrophil Dysfunction in HBV-Related Acute-on-Chronic Liver Failure. Front Immunol 2021;12:620365. doi:10.3389/fimmu.2021.620365, PMID:33717119.
[46] Zhao Q, Chen DP, Chen HD, Wang YZ, Shi W, Lu YT, *et al*. NK-cell-elicited gasdermin-D-dependent hepatocyte pyroptosis induces neutrophil extracellular traps that facilitate HBV-related acute-on-chronic liver failure. Hepatology 2025;81(3):917–931. doi:10.1097/HEP.0000000000000868, PMID:38537134.
[47] Liao F, Fan J, Wang R, Xu Z, Li Q, Bi W, *et al*. Neutrophil extracellular traps in sepsis: trade-off between pros and cons. Burns Trauma 2025;13:tkaf046. doi:10.1093/burnst/tkaf046, PMID:40904580.
[48] Falcinelli E, Petito E, Gresele P. The role of platelets, neutrophils and endothelium in COVID-19 infection. Expert Rev Hematol 2022;15(8):727–745. doi:10.1080/17474086.2022.2110061, PMID:35930267.
[49] Bonaventura A, Vecchié A, Dagna L, Martinod K, Dixon DL, Van Tassell BW, *et al*. Endothelial dysfunction and immunothrombosis as key pathogenic mechanisms in COVID-19. Nat Rev Immunol 2021;21(5):319–329. doi:10.1038/s41577-021-00536-9, PMID:33824483.
[50] Sung PS, Yang SP, Peng YC, Sun CP, Tao MH, Hsieh SL. CLEC5A and TLR2 are critical in SARS-CoV-2-induced NET formation and lung inflammation. J Biomed Sci 2022;29(1):52. doi:10.1186/s12929-022-00832-z, PMID:35820906.
[51] Das D, Thacker H, Priya K, Jain M, Singh S, Rai G. Complement component 5a receptor 1 and leukotriene B4 receptor 1 regulate neutrophil extracellular trap (NET) formation through Rap1a/B-Raf/ERK signaling pathway and their deficiency in term low birth weight newborns leads to deficient NETosis. Int Immunopharmacol 2024;142(Pt B):113165. doi:10.1016/j.intimp.2024.113165, PMID:39303536.